Transglutaminase 3 crosslinks secreted MUC2 and stabilizes the colonic mucus layer

Jack Sharpen
University of Manchester https://orcid.org/0000-0002-6268-3244
Brendan Dolan
University of Gothenburg
Elisabeth Nyström
University of Gothenburg
George Birchenough
University of Gothenburg https://orcid.org/0000-0003-2283-2353
Liisa Arike
University of Gothenburg
Beatriz Martinez-Abad
University of Gothenburg https://orcid.org/0000-0002-0521-3473
Malin Johansson
University of Gothenburg https://orcid.org/0000-0002-4237-6677
Gunnar Hansson
University of Gothenburg https://orcid.org/0000-0002-1900-1869
Christian Recktenwald (christian.recktenwald@medkem.gu.se)
University of Gothenburg https://orcid.org/0000-0003-1710-1863

Article

Keywords: colonic mucus layer, TGM3, transglutaminase, MUC2 mucin

Posted Date: June 21st, 2021

DOI: https://doi.org/10.21203/rs.3.rs-555255/v1

Version of Record: A version of this preprint was published at Nature Communications on January 11th, 2022. See the published version at https://doi.org/10.1038/s41467-021-27743-1.

Transglutaminase 3 crosslinks secreted MUC2 and stabilizes the colonic mucus layer

Jack D. A. Sharpen, Brendan Dolan, Elisabeth E. L. Nyström, George M. H. Birchenough, Liisa Arike, Beatriz Martinez-Abad, Malin E. V. Johansson, Gunnar C. Hansson and Christian V. Recktenwald*

From the Department of Medical Biochemistry, University of Gothenburg, SE-405 30 Gothenburg, Sweden

*Correspondence to: christian.recktenwald@medkem.gu.se

Abstract

The colonic mucus layer is organized as a two-layered system providing a physical barrier against pathogens and simultaneously harboring the commensal flora. The factors contributing to the organization of this gel network are not well understood. In this study, the impact of transglutaminase activity on this architecture was analyzed. Here, we show that transglutaminase TGM3 is the major TGM isoform expressed and synthesized in the colon. Furthermore, intrinsic extracellular TGM activity in the secreted mucus was demonstrated *in vitro* and *ex vivo*. Absence of this acyl-transferase activity resulted in faster degradation of the major mucus component the MUC2 mucin and changed the biochemical properties of mucus. Finally, TGM3-deficient mice showed an early increased susceptibility to DSS-induced colitis. Thus, these observations suggest that natural isopeptide cross-linking by TGM3 is important for mucus homeostasis and protection of the colon from inflammation, a suggested pre-stage of colon carcinoma.

Introduction

The epithelium in the intestinal tract is covered by mucus that provides protection from luminal challenges and bacterial infiltration [1]. Despite the similar proteome composition, the organization of the mucus gel network differs considerably in the small and large intestine [2]. Whereas small intestinal mucus is non-attached, the colonic mucus is a two-layered system with an attached, bacteria-free inner layer and an outer layer harboring the commensal flora [1, 3, 4]. The molecular mechanisms determining these structural differences are not well understood. The predominant component of mucus is the gel-forming MUC2 mucin that is synthesized by intestinal goblet cells. It has been shown that *Muc2*$^{-/-}$ mice develop spontaneous colitis, a pre-stage of colon carcinoma[5] [6]. Furthermore, the MUC2 levels in patients suffering from active ulcerative colitis (UC) are decreased when compared to healthy control patients [7].

The human MUC2 monomer consists of 5,130 amino acids organized in three complete and one partial von Willebrand D (VWD) domains in the N-terminal part followed by the first CysD domain and two Proline-, Threonine- and Serine-rich (PTS) sequences that are separated by the second CysD domain [8, 9]. The C-terminus harbors a fourth vWD domain, two vWC domains, and the cysteine-knot. During its transport through the endoplasmic reticulum and the Golgi-network MUC2 monomers first form C-terminal dimers and in the later stages of the secretory pathway N-terminal dimers or trimers[10, 11]. Furthermore, the PTS sequences become heavily *O*-glycosylated to form mucin domains. This posttranslational modification (PTM) shifts the mass of MUC2 from roughly 650 kDa to more than 2.5 MDa. During the later stages of the secretory pathway isopeptide bonds are introduced probably contributing to the insolubility of MUC2 in chaotropic salts, like guanidinium chloride [12]. An enzyme family that is able to catalyze these natural protein cross-links are transglutaminases (TGM).

Transglutaminases (R:protein-glutamine γ-glutamyltransferases; E. C. 2.3.2.13) comprise a family of Ca^{2+}-dependent acyl-transferases that can catalyze the transamidation or deamidation of protein-bound glutamine residues that can lead to natural cross-links through the formation of an isopeptide bond between the side chains of glutamine and lysine. This PTM is known to limit protein degradation by conformational changes and modification of protease-labile Lys residues [13, 14]. There are nine mammalian TGMs where TGM2 is the most ubiquitously expressed isoform [13, 15]. This isoform is predominantly localized in the cell cytosol, but can also be found associated with the plasma membrane. Furthermore, it can be secreted by unknown mechanisms after P2X7 receptor activation [16]. The enzymatic activity of TGM2 is normally silent but during mechanical injury it becomes activated and acts as a wound healing enzyme by stabilizing extracellular matrix (ECM) and cell-ECM interactions [17, 18]. Another process where TGMs are important is the morphogenesis of the skin. Here, TGM1, 3 and 5 are involved in the formation of the stratum corneum by cross-linking the envelope precursors such as inloricrin and involucrin [19].

Whether transamidation also has a role in the formation and stabilization of intestinal mucus is currently unknown. Mucus and mucins are stored highly concentrated in the granules of goblet cells and expand 1,000-fold in volume upon secretion. If TGM-catalyzed isopeptide cross-links contribute to mucus homoeostasis, this processing has to occur after secretion and expansion. Here, we suggest that extracellular TGM activity plays a role in organizing the mucus gel in the colon, especially by increasing its stability. To test this hypothesis the abundance of different TGM isozymes was evaluated and their enzymatic activity determined. We found that the formation of N^{ε}-(-γ-glutamyl)-lysine isopeptide cross-links in colonic mucus was based on extracellular TGM3-intrinsic activity. Furthermore, mice lacking this TGM isoform secrete a more protease-sensitive MUC2 molecule. In addition, *Tgm3*$^{-/-}$ mice are less protected against dextran sodium sulfate (DSS) induced

colitis. Together, our observations indicate that TGM-catalyzed cross-links are important for the stabilization/homoeostasis of colonic mucus and its resistance against disease-inducing conditions.

Results

Transglutaminase TGM 3 is a dominant cross-linking enzyme in the colon

Firstly, we determined which transglutaminase isozymes were expressed and synthesized in the colonic epithelium. Mouse colon tissue of wild-type (WT) and *Tgm* knock-out mice were analyzed for protein abundance by using immunohistochemistry (IHC), mass spectrometry (MS) and gel electrophoresis followed by western blot. As we were interested on the impact of transglutaminases on mucus homeostasis a recently published single cell transcriptomic study[20] analyzing MUC2-producing goblet cells and non-goblet epithelial cells was mined for the expression profile and protein abundance of the various TGM family members. Analyzing mRNA levels in colonic goblet cells and the remaining epithelial cell populations revealed only transcripts for *Tgm*2 and *Tgm*3 genes (Fig. 1a). Next, the TGM2 and TGM3 protein abundance determined by mass spectrometry (MS) in these two cell fractions was extracted. This method revealed approximately 10-times lower levels of TGM3 in the goblet cells compared to the non-goblet epithelial cells whereas the abundance of TGM2 was two-three orders of magnitude lower than TGM3 in the respective cell population (Fig. 1b). To evaluate the tissue localization of TGM2 and TGM3, immunohistochemical analyses were performed in WT, *Tgm*2$^{-/-}$ and *Tgm*3$^{-/-}$ animals together with the UEA1 lectin staining for the highly glycosylated MUC2 mucin. None of the strains reacted with the anti-TGM2 antibody, confirming the low levels of this isoform (Fig. 1c). That this antibody was functional was tested on duodenal tissue sections where a signal for TGM2 was easily observed (Suppl. Fig. S1a). In line with the quantitative data from mRNA expression and protein abundance, both

WT and *Tgm2*$^{-/-}$ animals showed a strong staining for the TGM3 isoenzyme in the epithelium and as expected no signal in *Tgm3*$^{-/-}$ mice (Fig. 1d).

As TGM3 lacks a signal sequence, we determined if TGM3 could nonetheless be secreted into the mucus. To answer this, gel electrophoresis and western blot analyses for TGM2 and 3 in colonic mucus were performed. Recombinantly expressed TGM2 and cleaved TGM3 were also loaded as positive controls either non-activated or activated by Ca^{2+}-preincubation (Fig. 1e). The majority of TGM3 was represented by a band migrating around 75 kDa and a weaker signal migrating at approximately 50 kDa in both WT and *Tgm2*$^{-/-}$ animals. These two bands represent the zymogenic and active form of the enzyme, respectively. Furthermore, several diffuse, but weak, TGM3-signals migrating between 150 and 250 kDa were detected in the WT and *Tgm2*$^{-/-}$ strains suggesting the self-multimerization of the enzyme and/or its incorporation into substrate proteins. As similar signals were detected in the activated positive control for TGM3, it is likely that self-multimerization occurs in mucus. In contrast, TGM 2 was not detected in the mucus samples of any mouse strain. Specificity of the used antibodies for the respective isoform was determined upon western blot analyses, the anti-TGM3 antibody showed a cross-reactivity <8 % on TGM2 and similarly vice versa (Suppl. Fig. S1b) Together the results show that TGM3 is the predominant transglutaminase in the colonic epithelium and the only isozyme detected in the mucus. Furthermore, its expression in goblet cells suggests that its presence in mucus arises at least partly from active secretion and not only from shedded cells.

TGM3 activity is present in colonic mucus

Next, we asked if TGM3 is enzymatically active in the colonic mucus and could thereby contribute to its stability by the formation of additional cross-links. For that purpose, a qualitative assay using the incorporation of biotinylated isoform-specific substrate peptides

126 T26 (TGM2) and E51 (TGM3) in mucus was performed. The mucus was incubated with Ca^{2+}
127 and the respective peptide probe followed by gel electrophoresis and western blot using
128 streptavidin detection (Fig. 2a). Specific incorporation of the two peptides was observed in
129 WT and *Tgm2*$^{-/-}$ mucus, but not in mucus from *Tgm3*$^{-/-}$ animals. Non-specific signals were
130 observed in all samples, including control reactions where transglutaminase activity was
131 inhibited by iodoacetamide (IAA). These bands are likely due to endogenously biotinylated
132 proteins as for example pyruvate-carboxylase. Thus, the detected cross-linking activity in the
133 mucus arises from TGM3-mediated catalysis. To analyze if endogenous mucus contains
134 sufficient Ca^{2+}-ions for the activation of TGM3, the experiment was repeated without
135 calcium addition. Similar results as with exogenous Ca^{2+}-addition were obtained, indicating
136 the presence of intrinsic extracellular transglutaminase activity in colonic mucus (Fig. 2b).
137 These results suggest that endogenous acyl-donor protein substrates are present in colonic
138 mucus. However, the formation of a transglutaminase-catalyzed cross-linked mucus gel-
139 network also requires the presence of acyl-acceptor proteins. Therefore, the Ca^{2+}-free
140 experimental set up was modified by replacing the glutamine-donor with the primary amine
141 5-Biotinyl-pentylamine (5-BP) as acyl-donor. Similar to the results from the acyl-acceptor
142 experiments, specific signals were detected when the acyl-donor compound was added to
143 mucus of WT and *Tgm2*$^{-/-}$ animals, but not in the *Tgm3*$^{-/-}$ mucus or when IAA was added
144 (Fig. 2c). Together, the results show that colonic mucus contains intrinsically, active TGM3
145 as well as both acyl-acceptor and –donor molecules allowing transamidating reactions to take
146 place.

147 To quantify the intrinsic transamidating activity in colonic mucus, a colorimetric assay
148 for the incorporation of a TGM-promiscuous peptide (A25) and the two isozyme-selective
149 peptide substrates (peptides T26[21] and E51[22]) into casein was performed (Fig. 2d). A natural
150 cross-linking activity in WT mucus of ≈ 8±2 U/mg for the promiscuous substrate was

151 determined. Substitution with the TGM3-specific substrate E51 led to a 1.5-fold increase
152 (≈12 ± 4 U/mg) of the transamidating activity, whereas a residual activity of 0.8 ± 0.3 U/mg
153 was observed for the TGM2-specific substrate. However, no measurable activity could be
154 obtained in the *Tgm3*$^{-/-}$ mucus as the detected values were below the limit of detection for our
155 assay (Fig. 2d, Suppl. Fig. S2). Blocking of the TGM-reaction with Z-DON led to an almost
156 complete (88%) inhibition for the promiscuous peptide A25. In line with our other results
157 (Fig. 1, Fig. 2 a-c), the natural cross-linking activity was related to TGM3 as the use of the
158 TGM2-specific substrate T26 led to less than 10% transglutaminase activity compared to the
159 TGM3-specific substrate in WT animals and was also below the limit of quantification of this
160 assay. These experiments further demonstrated substantial intrinsic transamidating activity in
161 colonic mucus of WT animals, but not in *Tgm3*$^{-/-}$, as addition of extra Ca^{2+} was not required.
162 The intrinsic mucus transamidating activity of TGM3 was further studied using an *ex*
163 *vivo* approach where the distal colon from WT and *Tgm3*$^{-/-}$ animals were mounted in a
164 perfusion chamber and the fluorescently labelled glutamine-donor probe E51 was added and
165 its incorporation monitored (Fig. 2e). Fig. 2f-h show the confocal microscopic analyzes of
166 E51 incorporation in the respective tissue/mucus specimen in the x/z plane (top panels) and
167 snap shots of probe incorporation of the x/y plane inside the mucus (bottom panels). A
168 homogeneous punctuated pattern of E51 fluorescence was observed throughout the whole
169 mucus layers of WT animals (Fig. 2f and Suppl. Movie M1). However, when *Tgm3*$^{-/-}$ mice
170 were analyzed in the same way, the incorporation was dramatically reduced and limited to
171 shedding epithelial cells (Fig. 2g). A similar lack of incorporation in WT animals was
172 observed in the presence of the transglutaminase inhibitor Z-DON (Fig. 2h). These results
173 demonstrate extracellular TGM3 activity *ex vivo*. Together these results show that the colonic
174 mucus contains natural acyl-donor and acyl–acceptor molecules together with intrinsic
175 TGM3-mediated transamidating activity.

Loss of TGM3 alters biochemical properties of mucus/MUC2

The MUC2 monomer is a large glycoprotein with a mass of around 2.5 MDa (Fig. 3a). It is the most abundant constituent in colonic mucus and is thus a potential target for TGM3-mediated cross-linking, something that could influence its biochemical properties. Colonic mucus from WT, *Tgm2*$^{-/-}$ and, *Tgm3*$^{-/-}$ mice was isolated and disulfide bonds reduced followed by separation via composite agarose-PAGE (AgPAGE) and detected by in-gel immunostaining using anti-MUC2C3 antibody (Fig. 3b). WT and *Tgm2*$^{-/-}$ showed two identical diffuse fast-moving bands assumed to be MUC2 monomeric bands and several additional slow-moving and heavily stained bands for higher oligomers. This was in contrast to the *Tgm3*$^{-/-}$-mucus, where MUC2 showed a faster migrating diffuse band and two to WT different bands migrating similar to the WT monomer.-These differences in the electrophoretic migration pattern suggest that *Tgm3*$^{-/-}$ MUC2 is qualitatively different to that of WT and *Tgm2*$^{-/-}$ and argues for TGM3-mediated isopeptide bond modification of MUC2.

As isopeptide bonds can prevent proteolytic cleavage and secreted mucus is normally exposed to numerous endogenous and bacterial proteolytic enzymes, we hypothesized that the different size of MUC2 formed in *Tgm3*$^{-/-}$ mice was a result of protease-catalyzed degradation *in vivo*. To test this hypothesis, colonic mucus of WT and *Tgm3*$^{-/-}$ mice was first isolated and solubilized by reduction with dithiotreitol. The resulting samples were treated with the serine protease LysC, followed by the separation of the reaction products via composite AgPAGE and Alcian Blue staining of the heavily glycosylated and protease-resistant MUC2 domains (PTS sequence). All three strains showed three identical intensely stained bands after LysC treatment (Fig. 3c). Interestingly, this band pattern was also observed in the non-treated *Tgm3*$^{-/-}$ mice, but not in the WT or *Tgm2*$^{-/-}$ animals. This could suggest that the faster migrating MUC2 bands in the non-treated *Tgm3*$^{-/-}$ animals represent products that have been already degraded *in vivo*. To confirm this, the fastest MUC2

migrating bands from the non-treated WT (WT-M) and *Tgm3*$^{-/-}$ (*Tgm3*$^{-/-}$-M) samples were excised from the gels (Fig. 3b) followed by mass spectrometric analyses of their tryptic/AspN peptides. The peptide coverage of the MUC2 sequence of three biological replicates is summarized in a heat-map shown in Fig. 3d. The WT monomers showed peptides from all domains except the PTS as expected. Interestingly, the *Tgm3*$^{-/-}$ MUC2 molecule showed almost exclusively peptides from the central CysD2 domain (Fig. 3a and d). The vWD4 domain was weakly covered in both animals explaining the anti-MUC2C3 staining. As the fastest migrating bands in the *Tgm3*$^{-/-}$ mucus were stained by Alcian Blue and have masses larger than 460 kDa, these bands must also include the two mucin domains surrounding CysD2. These PTS1 and PTS2 sequences are highly glycosylated, resistant to proteolytic enzymes, and not identifiable by mass spectrometry (Fig. 3a). Thus, the MUC2 mucin in the *Tgm3*$^{-/-}$ mice is suggested to be already degraded *in vivo* due to it being more susceptible to degradation in the colon lumen.

The most likely explanation for the more degraded MUC2 in *Tgm3*$^{-/-}$ mice is the loss of protective transglutaminase-catalyzed isopeptide bonds. To search for such bonds, we mined the mass spectrometry data sets for the presence or absence of such cross-links. An example is shown in the mass spectrum of a dipeptide for an intramolecular cross-link connecting Gln 2503 with Lys 2508 (Fig. 3e). This intramolecular cross-linked peptide was only detected in MUC2 from WT, but not in *Tgm3*$^{-/-}$ animals. This isopeptide bridge is located between the vWC2 domain and the cysteine-knot (CK) domain (Fig. 3a). There are likely several additional cross-links and this isopeptide-bridged peptide is only one example, but its absence in *Tgm3*$^{-/-}$ MUC2 supports this interpretation.

As non-reduced secreted MUC2 polymers in the intestine are known to be insoluble in guanidinium chloride due to isopeptide bonds formed intracellularly [23], we asked if TGM3-mediated isopeptide cross-links contributed to this property. To address this question,

insoluble mucus from WT and *Tgm3*$^{-/-}$ mice was precipitated by centrifugation and the turbidity of soluble material in the supernatant recorded (Fig. 3f). The turbidity of the samples from *Tgm3*$^{-/-}$ animals was increased by approximately 30 % when compared to WT and *Tgm2*$^{-/-}$ strains. This result further supports the idea that disintegration of the MUC2 mucin network was more prominent in the mice lacking the TGM3 enzyme.

Mucins have been shown to attach to hydrophobic surfaces [24]. We hypothesized that natural isopeptide cross-links might contribute to this biophysical property and thus analyzed the hydrophobic character of colonic mucus by using a thermal fluorescent shift assay. Colonic mucus mixed with the hydrophobic dye SyproOrange was subjected to a linear temperature gradient and the fluorescence measured (Fig. 3g). At higher temperatures (>50˚C) the *Tgm3*$^{-/-}$ mucus showed an increased fluorescence in relation to WT, indicating an increased exposure of hydrophobic protein parts. Preincubation of *Tgm3*$^{-/-}$ mucus with recombinant TGM3 partly normalized the mucus. It can be suggested that TGM3-mediated isopeptide bonds in WT mucus prevented the unfolding of its constituents.

Mucus processing and tissue secretory responses were assessed using *ex vivo* mucus measurement assays. Using this approach, we detected no differences in baseline mucus growth rate or carbachol-induced secretory responses between WT and *Tgm3*$^{-/-}$ tissues (Suppl. Fig. S3a). A similar approach can be used to measure mucus barrier function by applying bacteria-sized (1µm diameter) beads to the mucus surface and determining the extent of bead penetration into the mucus *via* confocal microscopy. However, again no difference between WT and *Tgm3*$^{-/-}$ tissues was detected using this approach (Suppl. Fig. S3b), which was surprising, as we had observed a more degraded MUC2 mucin in the *Tgm3*$^{-/-}$ animals. Nonetheless, we hypothesized that lack of TGM3 would affect mucus barrier stability and thus treated colonic tissue from WT and *Tgm3*$^{-/-}$ animals with pronase. In WT animals and before addition of pronase to *Tgm3*$^{-/-}$ tissue, the fluorescent beads remained on

top of the mucus layer (Fig. 3h and Suppl. Movies M2 and M3). However, after pronase-treatment of *Tgm3*$^{-/-}$ explants, a progressive decrease in mucus thickness was observed and the beads were more easily washed away and/or penetrated down to the epithelial surface indicating that *Tgm3*$^{-/-}$ mucus was less protected against proteolytic attack (Fig. 3i and Suppl. Movie M3).

Tgm3$^{-/-}$ *mice are more susceptible to early DSS-induced damage*

The altered biochemical properties of mucus and its higher susceptibility to proteolytic degradation in the absence of TGM3 activity suggested that *Tgm3*$^{-/-}$ mice could be more susceptible to dextran sodium sulfate (DSS) induced colitis. To test this, age-matched cohoused *Tgm3*$^{-/-}$ and WT animals were challenged with DSS. The body weight of WT mice increased during the first four days whereas the *Tgm3*$^{-/-}$ animals started to lose weight from day three and showed on trend decreased body weights compared to WT mice until day 6 (Fig. 4a). This was reflected by an earlier detection of occult blood in the feces of *Tgm3*$^{-/-}$ mice one day after the start of the experiment (Fig. 4b). Consequently, the *Tgm3*$^{-/-}$ animals showed a significant raised disease activity index score (DAI) from day two to day five after the start of the DSS-treatment (Fig. 4c). Higher DAI was maintained in the *Tgm3*$^{-/-}$ compared to WT animals until day 6, when the colitis became also established in the WT animals. Finally, 50% of the *Tgm3*$^{-/-}$ animals had to be sacrificed at day 7, compared to 10 % of WT mice, due to suffering and loss of weight following the ethical permit (Fig. 4d). Furthermore, the colon length of *Tgm3*$^{-/-}$ mice was reduced to 88% of the WT length after 7 days of DSS treatment (Fig. 4e and f). Histopathological analysis of the colonic tissue after eight days of DSS treatment revealed the loss of crypts and an extensive infiltration of immune cells in both strains. These effects were more pronounced in the distal colon (Fig. 4g). However, histological examination of Hematoxylin/Eosin-stained tissue by a blinded pathologist did not

detect significant differences between the two animal strains at the end of DSS-treatment (not shown). DSS has previously been shown to disrupt the mucus layer properties [25] and mice lacking the MUC2 mucin are very susceptible already at day one of DSS treatment[4]. The early on-set of DSS effects in the *Tgm3*$^{-/-}$ supports the conclusion that the colonic mucus is defect in these animals. When colonic tissue was analyzed by immunohistochemistry for TGM2, this isozyme that was absent in non-treated WT and *Tgm3*$^{-/-}$ as shown in Fig. 1a, was now detected in both the WT and *Tgm3*$^{-/-}$ animals after 7 days of DSS-treatment (Fig. 4h). Taken together *Tgm3*$^{-/-}$ animals were significantly more susceptible towards the colitis-inducing effects of DSS as a faster disease onset was observed resulting in a decreased probability of survival.

Discussion

We have previously shown that the reduction-insensitive MUC2 oligomers formed in a cell line producing MUC2 were cross-linked by isopeptide bonds as catalyzed by a yet unidentified transglutaminase [12]. However, this colorectal cell line does not secrete MUC2 and could not be used to learn if and how extracellular cross-linking could contribute to mucus homeostasis and colon barrier function. By using WT and knock-out mouse strains, we uncovered intrinsic transglutaminase activity in secreted colonic mucus mediated by TGM3. The observations provide evidence for the protective effect by natural cross-links. That TGM3 is the dominant transglutaminase of the colon is in accordance with a previous mucus proteome study [2]. mRNAseq and MS studies detected minor amounts of TGM2, but based on the label-free mass spectrometric quantification TGM2 was <1% of that of TGM3 and could represent contaminating material from the ileum. In support of this, TGM2 was not detected by immunohistochemistry or gel electrophoresis/western blot. Previous work from Jeong and co-workers has claimed TGM2 as the major transglutaminase of the colon [26].

However, these authors used only immunohistochemistry to demonstrate the presence of TGM2 and no antibody staining against TGM3 was tested. Likely cross reactivity of the used antibody can explain this observation.

The strong TGM3 signals observed by gel electrophoresis/western blot analyses of mucus represented the zymogenic form of TGM3. In addition to this, several TGM3 bands with higher molecular masses were detected in the range between 150 and 250 kDa. Together with control reactions performed with recombinantly activated TGM3, these signals strongly suggest that the enzyme can self-multimerize and/or incorporate itself into other molecules as previously observed for TGM2 [27].

Recent reports have shown that TGM2 is extracellularly inactive and can be activated after injury or stress [17, 28]. Here, we were able to demonstrate intrinsic, extracellular transglutaminase activity in both the WT and *Tgm2*$^{-/-}$ mouse strains, but its absence in *Tgm3*$^{-/-}$ animals. In addition, the obtained information showed the presence of natural acyl-donor and –acceptor molecules in colonic mucus thereby implying the possibility of *in vivo* isopeptide-based cross-linking of different mucus components. Furthermore, transglutaminase activity could be detected without calcium-addition, showing that extracellular transglutaminase activity is intrinsic to the large intestinal mucus. Since a >90 % reduction in TGM activity was observed when the TGM2-selective substrate T26 was used in a quantitative assay and no activity was found in the *Tgm3*$^{-/-}$ animals, we can conclude that the transamidation activity of mucus is almost exclusively dependent on TGM3 in colon. This is in line with the shown absence of TGM2 protein. In an *ex vivo* assay, a punctated incorporation of the specific TGM3 peptide substrate E51 in colonic mucus was observed confirming our *in vitro* observations. However, it was not possible to perform the *ex vivo* mucus incorporation approach under Ca^{2+}-free conditions since the normal cellular signaling of the tissue depends on an extracellular calcium pool. This is reflected by measurements of the luminal calcium

concentrations in the gut which vary between 5 and 20 mM depending on the feed state [29, 30] whereas the concentration in the used buffer was 1.3 mM representing the physiological luminal calcium concentration [31]. Given that only 20% of the daily calcium intake is resorbed, mainly in the small intestine, the luminal Ca^{2+}-concentration in the colon should be sufficient to occupy the second and third Ca^{2+}-binding site of TGM3 necessary for its activation [32, 33]. Furthermore, TGM3 is expressed and synthesized in goblet cells, a secretory cell lineage whose secretory granules contain high calcium concentrations for the packing of the MUC2 mucin. Secretory granules can contain calcium concentrations of up to 40 mM [34]. The pH in goblet cell granule is acidic and the Ca^{2+}-ions are bound to MUC2 and the other stored molecules. After secretion, the pH raises, and free Ca^{2+}-ions will become available. For the activation of TGM3, the Ca^{2+}-binding sites must be occupied and the zymogenic form of TGM3 needs to be cleaved in the loop harboring amino acids 462-469. For this to take place, Cathepsin L or S have been suggested as activating proteases [35]. Interestingly, Cathepsin S is a core mucus component and Cathepsin L is also expressed in colonic epithelial and goblet cells [7] and Suppl. Fig. S4. This suggests that TGM3 can become fully activated in the colonic mucus and lumen, in line with the endogenously observed TGM3 activity in colon mucus. Overall, the availability of calcium and Cathepsin S and L together with an alkaline pH in the large intestinal lumen provide favorable conditions for TGM3 to catalyze transamidating reactions in colonic mucus.

The observed intrinsic, extracellular transglutaminase activity led us speculate about the putative functional impact of the natural cross-links in colonic mucus. The comparison of mucus from WT and *Tgm3*$^{-/-}$ mice provided direct experimental evidence that the loss of TGM3 led to important biochemical alterations of the dominant mucus skeleton protein MUC2. We observed an extensive degradation of the polypeptide as the N-terminal part with the first three vWD and the first CysD domain was lost comprising approximately 1,300

amino acids as well as most of the C-terminus. Thus, leaving a central part of the MUC2 mucin consisting of the two highly glycosylated PTS sequences connected via the second CysD domain behind. The resistance of the mucin domains to proteolytic cleavage is due to their dense decoration by *O*-linked glycans resulting in steric hindrance to protease degradation. Another feature of MUC2 that was affected in *Tgm3*$^{-/-}$ mice is its solubility. MUC2 polymers become insoluble during their transport through the later stages of the secretory pathway [23]. In our turbidity assay, an effect on the MUC2 gel network was indicated by an increased optical density in the mucus supernatant from *Tgm3*$^{-/-}$ mice. This suggests more soluble MUC2 in this mouse strain. In addition to its solubility, the hydrophobicity of MUC2 was also altered in the absence of TGM3. The assay showed an increased exposure of hydrophobic patches in partly purified MUC2 from *Tgm3*$^{-/-}$ animals compared to WT animals upon heat-induced denaturation. This may reflect that the N$^{\epsilon}$(-γ-glutamyl)-lysine bonds in WT-MUC2 stabilize the protein. This phenomenon was partly reverted by preincubating the *Tgm3*$^{-/-}$ mucus with recombinant TGM3, supporting the impact of isopeptide bonds on this biophysical parameter. Our observations are consistent with previous studies showing that isopeptide bonds can stabilize bacterial pili proteins in this kind of assay [36, 37]. However, the insoluble nature of the MUC2 mucin makes it impossible to purify the MUC2 polypeptide in its native conformation, making recording of a specific melting temperature impossible.

In the *Tgm3*$^{-/-}$ mice, the shortened and more degraded MUC2 still seems to be sufficient to provide enough protection for the colonic epithelium. This mouse strain behaves normally and shows no obvious signs of colon inflammation under normal conditions. It is likely that the highly *O*-glycosylated mucin domains of MUC2 are sufficient to trap microorganisms and prevent bacteria from reaching the epithelial cells. However, challenging the system by the addition of a mixture of serine proteases deciphered an altered phenotype in *Tgm3*$^{-/-}$ animals

376 in an *ex vivo* bead penetration assay. In this approach, the mucus layer seemed to be more
377 disintegrated and less organized allowing the bacteria-mimicking beads to reach the
378 epithelium suggesting a compromised barrier function. We also obtained direct experimental
379 support of this hypothesis by administering DSS to WT and *Tgm3*$^{-/-}$ animals. DSS quickly
380 disintegrates the inner colon mucus layer allowing bacteria to reach the epithelium and
381 trigger inflammation typically observed after five days [25]. DSS treatment showed that the
382 *Tgm3*$^{-/-}$ mice were more susceptible and showed defects already after only two days of
383 treatment. The early onset suggest direct effects on mucus that are likely explained by the
384 decreased inter-molecular cross-links in the mucus of *Tgm3*$^{-/-}$ mice. Less cross-links will, as
385 shown here, make the mucus more susceptible to proteolytic degradation and detachment
386 leading to a faster mucus removal by intestinal peristalsis. Interestingly, two transcriptomic
387 studies using either the 2,4,6-trinitrobenzene sulfonic acid or the adoptive T-cell transfer
388 colitis model detected TGM3 downregulation after the establishment of the disease, thereby
389 suggesting an impact of this enzyme for a healthy gut[38, 39]. In contrast to non-treated mice,
390 both the WT and *Tgm3*$^{-/-}$ mice synthesized the TGM2 enzyme in their colonic mucosa after
391 DSS treatment. This might reflect a role for TGM2 in wound healing as suggested previously
392 [18, 26]. As mucus can be regarded as our 'inner skin' it is not surprising that a weakened mucus
393 barrier in the *Tgm3*$^{-/-}$ mice could be regarded in analogy with the TGM3 function in the skin
394 where earlier observations have shown that these animals have an impaired skin barrier [40].
395 This study identifies TGM3 as an important natural cross-linking enzyme acting on the
396 expanded secreted mucus and by this contributing to the stabilization of the colonic mucus
397 gel network. The MUC2 mucin and other mucus components are secreted into the harsh
398 luminal environment where proteases from the host, the commensal bacteria, and eventually
399 from pathogens reside. The TGM3-catalyzed formation of isopeptide bond cross-links
400 strengthens the mucus barrier and thereby increase the mucus protection of the colonic

epithelium. However, further studies are required to more precisely understand the molecular details for the role of transglutaminases for the mucus structure. For example, as there exists an inverse gradient of TGM2 and 3 abundance from the small to the large intestine it would be interesting to determine the activity of TGM2 and decipher its role for small intestinal mucus. Our observations increase our understanding of the molecular mechanisms that contribute to the architecture of the colonic mucus layers and suggest potential treatment options for the human disease UC.

Methods

*Animal*s

C57/BL6N mice were from Taconic. *Tgm*2$^{-/-}$ mice[41] were provided from Oslo University Hospital (Norway). *Tgm*3$^{-/-}$ mice[42] were obtained from the University of Rome (Tor Vergata, Italy). All animal experiments were conducted according to the Swedish legislation (Jordbruksverket; Ethical permits no.: 2285/19 and 2292/19). Mice were maintained at 22˚C with light/dark cycles of 12 hours each. Animals received a standard rodent diet and water was supplied *ad libitum*.

Antibodies, enzymes, chemicals

If not otherwise specified chemicals were bought from Sigma. For the detection of TGM2 the monoclonal CUB7402 antibody (Thermo Fisher Scientific) was used for both immunohistochemistry (IHC) and Western Blot. TGM3 detection was performed using the polyclonal NBP1-57678 antibody (Novus Biologicals) for both applications. Cross-reactivity of the two antibodies was analysed by western blot against recombinant TGM2 and 3 (Suppl. Fig. S1b). For IHC detection of TGM2 a goat-α-mouse-IgG1 antibody coupled to AlexaFluor647 (Invitrogen) and a goat-α-rabbit-IgG antibody coupled to AlexaFluor647

(Invitrogen) for TGM3 detection was used. For Western Blot detection of TGM2 a goat-α-mouse-IgG1 antibody coupled to the IRdye 680LT (LI-COR and a goat-α-rabbit-IgG antibody coupled to AlexaFluor 790 (Invitrogen) was used. Trypsin and AspN were from Promega. LysC was from WAKO (Japan). Recombinant TGM2 (T022) and TGM3 (T013) as well as the biotinylated glutamine donor substrates A25 (B001); T26 (B008); E51 (B009) and the biotinylated amine donor compound pentylamine (B002) were bought from Zedira (Germany). The FITC-labelled E51 probe was bought from CovalAb (France). Pronase was from Merck (Germany). The UEA1 lectin was from BioNordika.

Immunohistochemistry

Paraffin-embedded tissue sections were deparaffinized with xylene and rehydrated in ethanol solutions ranging from 100 % to 30 %. Antigen-retrieval was performed by boiling the sections in 10 mM citrate buffer pH 6.0. The sections were blocked for one hour with 5 % fetal bovine serum (FBS) in PBS. Afterwards the antibodies for TGM2 and 3 were added (1:200 diluted in PBS containing 5 % FBS) and the sections incubated overnight at 4˚C in a humid chamber followed by three washing steps in PBS. Secondary antibodies coupled to the AlexaFluor647 dye (α-mouse-IgG for TGM2 α-rabbit-IgG for TGM3, 1:1,000 diluted in PBS containing 5 % FBS) were added together with the UEA1 lectin (10 µg/ml) conjugated to the rhodamine dye for one hour. After three washing steps in PBS the nuclei were stained with the Sytox green stain for five minutes. After one additional washing step the sections were mounted using ProLong Gold-Antifade mountant (Thermo Fisher Scientific) and visualized by confocal microscopy (Zeiss Examiner 2.1; LSM 700).

Transglutaminase activity assays

Mucus supernatants (30 µg) were incubated either with 10 µM of the TGM2- or TGM3-specificic glutamine-donor peptides T26[21] or E51[22] or the amine-donor compound 5-Biotinyl-pentylamine for one hour at 37 ˚C. Control reactions were performed in the presence of 25 mM IAA and the respective compounds. The reactions were stopped by the addition of SDS-loading buffer and heating to 95˚C for five minutes. Reaction products were separated by SDS-PAGE on 4-15% gradient gels followed by semidry transfer to PVDF membranes. After blocking with 3% BSA in TBS buffer the membrane was incubated with streptavidin coupled to AlexaFluor 680 (1:20,000, Invitrogen) and the incorporation of substrates revealed on an Odyssey Li-COR Clx workstation.

Quantitative determination of TGM activity was performed according to the method described by Trigwell and coworkers[43]. Briefly, maxisorb 96-well plates (Thermo) were coated with 250 µl of a 0.1% casein solution in 50 mM sodium carbonate pH 9.8 for 12 hours. After emptying and washing 250 µl blocking solution (0.1% BSA in 50 mM sodium carbonate pH 9.8) was added and incubated for one hour at 37˚C. After washing, 150 µl reaction buffer (100 mM TrisHCl pH 8.5, 6.7 mM $CaCl_2$, 13.3 mM DTT containing either 10 µM biotinylated TGM-substrate peptide E51; T26, respectively or 5 µM biotinylated TGM-substrate peptide A25) for the respective TGM standards was added to the wells. For the analysis of mucus samples, DTT and calcium were omitted in the reaction buffer. Measurements were carried out in triplicate per biological replicate. The reactions were started by the addition of either 50 µl TGM standards (0; 25; 50; 75; 100; 125 mU/well) or mucus samples and incubated for one hour at 37˚C on a rotational shaker set to 100 rpm. Afterwards, the reactions were stopped by emptying the wells and washing. The incorporation of the substrates in the casein matrix was probed by the addition of 200 µl Extravidin solution (Extravidin-peroxidase (1:10,000 in 100 mM TrisHCl pH 8.5 containing

1% BSA) for one hour and gentle shaking. Biotin-Extravidin binding was visualized by adding 200 µl TMB developing solution (3,3´,5,5´-Tetramethylbenzidine, Sigma) and the reaction stopped by adding 50 µl 5 M H_2SO_4. The absorbance of reaction and standard wells was recorded at 450 nm on a Victor2 Wallac work station (Perkin Elmer). The activities of the samples were subsequently normalized against the protein content of the sample using the BCA method.

Ex vivo analysis of transglutaminase activity

Mice were anaesthetized using isofluorane and sacrificed by cervical dislocation. The colon was collected by dissection and flushed for the removal of intestinal content using Krebs buffer as previously described[44]. After removal of the muscle layer by microdissection the tissue was mounted in an in-house built horizontal chamber allowing basolateral perfusion with Krebs-Glucose buffer and apical Krebs-mannitol buffer (Fig. 2e). Two µM FITC-labelled E51-probe in Krebs-mannitol buffer was added and the tissue incubated for 30 minutes at 37˚C. Afterwards, non-incorporated probe molecules were washed away with Krebs-mannitol buffer followed by analysis of incorporation of the TGM3-substrate peptide on an upright LSM700 confocal microscope (Carl Zeiss, Germany) equipped with a 20x immersion lens (Pan-Apochromat 20x/1.0 DIC 75 mm; Carl Zeiss, Germany). Images were acquired using Zen Black software (Carl Zeiss) and z-stacks were exported to TIFF format using the Imaris software. Inhibition of transglutaminase activity in WT mice was achieved by adding 5 µM Z-DON (Zedira) together with the TGM3 substrate.

Ex vivo mucus integrity assay

Tissue was collected as described for the *ex vivo* analysis of transglutaminase activity. Following mounting in the perfusion chamber, tissue was stained with Syto 9 (1:500 in

Kreb's-mannitol buffer; Thermo Fisher) and the mucus layer was visualized by the addition of 1 µm fluorescent beads (Thermo Fisher). 20 mg/ml of pronase was added to the apical Krebs-mannitol buffer and the integrity of the mucus layer was monitored on an upright LSM900 confocal microscope (Carl Zeiss) using a water Pan-Apochromat 20x/1.0 DIC 75 mm lens (Carl Zeiss; Germany). Tissue explants were maintained at 37°C throughout the experiments. Briefly, z-stacks were acquired every 5 minutes (total time 1 hr.) using Zen Blue software (version 3.1; Carl Zeiss, Germany). In order to monitor mucus integrity beads and tissue surfaces were mapped to isosurfaces using Imaris software as described previously[45], data regarding the position of the fluorescent beads in relation to the tissue surface over time was then extracted and analyzed to generate normalized positional data over time (Prism version 9.1.0, Graphpad).

Colitis induction by DSS

Age- and sex-matched WT C57/BL6 and *Tgm3*$^{-/-}$ mice were cohoused for 4 to 5 weeks. Colitis was induced by adding 3% (w/v) dextran sodium sulfate (DSS) to the drinking water. Mice could drink *ad libitum*. The mice were sacrificed after eight days or if their body weight dropped by 10% from the initial weight. The probability of survival was defined when mice died or if they showed a body weight loss >10%. The colon was dissected and its length measured from cecum to anus and subsequently normalized against the initial body weight of the respective animal. Afterwards, the colon was flushed with PBS for the removal of fecal content. The colons were fixed as Swiss rolls in 4% paraformaldehyde and stained for hematoxylin/eosin and Alcian Blue-PAS. The disease activity index (DAI) was calculated as the sum of the combined scores for stool consistency, hematochezia and weight loss according to the methods of Friedman and co-workers[46]. The detection of occult blood was

524 performed using a Hemocccult kit (Beckman Coulter) according to the manufacturer`s
525 instructions. Two litters of each mouse strain with five animals per litter were analyzed.
526
527 *Composite agarose-PAGE*
528 The separation of MUC2 was performed according to the protocol of Schulz and coworkers[47].
529 Briefly, mucus was scraped from mouse colon and emulsified in TBS. Mucus/Muc2 was
530 precipitated by centrifugation at 16,000 x g and 4˚C for 30 minutes. The mucus was
531 solubilized by the addition of reducing gel-loading buffer (62.5 mM TrisHCl pH 6.8, 2%
532 SDS, 50 mM DTT 10% (v/v) glycerol). 67 µg were separated via AgPAGE for 3.5 h at 30
533 mA. The gels were either stained with Alcian Blue or MUC2 was detected by in-gel
534 immunodetection. For in-gel immunodetection, the gels were fixed in 50% (v/v) 2-Propanol/
535 5% (v/v) acetic acid for 15 minutes and gentle shaking followed by 30 minutes washing in
536 water. The primary antibody against MUC2 (Genentech; 1:500) was added for 12 hours at
537 4˚C in PBS-T buffer containing 5% BSA. After three washing steps with PBS-T for 10
538 minutes each, the secondary antibody α-rabbit-IgG-Licor790 (LiCOR, 1:5000) was added for
539 one hour at ambient temperature. After three to five extensive additional washing steps, the
540 immunostained gel was scanned with a LiCOR Clx instrument.
541
542 *Thermofluor assay*
543 Mucus from the indicated mouse strains was scraped from their distal colons and emulsified
544 in TBS buffer. Insoluble mucins were washed twice in TBS and recovered by centrifugation
545 (16,000 x g; 4˚C; 30 minutes). The protein concentration of the supernatant was determined
546 and the mucus pellet emulsified to a concentration of 1 mg/ml in each sample. 45 µl of
547 sample or TBS control were mixed with five µl of a 200-fold stock solution of SyproOrange
548 (Molecular Probes) and subjected to an increasing temperature gradient of 0.5˚C every 30

549 seconds from 25 to 99˚C in a CFX96 Real-time system (BioRad). The fluorescence was
550 recorded every 30 seconds and the fluorescence intensity of the TBS control subtracted. To
551 rescue the properties of mucus from WT mice 1 U recombinant TGM3 and 4 mM $CaCl_2$ were
552 applied to the mucus from *Tgm3*$^{-/-}$ mice and incubated for one hour at 37˚C. The reaction was
553 terminated by the addition of 5 mM IAA. The buffer controls for this part of the experiment
554 were treated accordingly and the melting curve recorded as described above. Three biological
555 replicates were analyzed in technical triplicates.
556
557 *Analysis of MUC2 depolymerization by turbidity measurement*
558 Scraped mucus samples were adjusted to 1 mg/ml and precipitated by centrifugation (1,000 x
559 g, 30 minutes, 4˚C). Afterwards, the turbidity of the supernatant was recorded at 600 nm
560 wavelength in a Spectramax photometer.
561
562 *Single cell transcriptomic analysis*
563 Goblet cells and non-goblet cells from the RedMUC2 reporter mouse strain were isolated by
564 FACS as described recently[20]. The used bulk RNA-seq data (GSE144363) are deposited in
565 GEO and belong to the superserie GSE144436. The quality of the data was assessed with
566 FastQC (version 0.11.2) and filtered using Prinseq (version 0.20.3). The reads were aligned
567 against the mouse reference genome mm10 with STAR (version 2.5.2b) and the number of
568 mapped reads was calculated with HTseq (version 0.6.1p1). Data normalization, differential
569 expression and statistical analysis were made with DESeq2 (version 1.14) in R.
570
571 *In-gel digestion and mass spectrometric analyses*
572 Protein bands of interest were excised from the gel and washed with 50 % acetonitrile and
573 dried in a vacuum centrifuge followed by reduction with DTT and alkylation with IAA.

Trypsin was added at a ratio of 1:50 and the samples incubated for 12 hours at 37˚C. Afterwards, AspN was added at a ratio of 1:50 and the samples incubated for additional 5 hours at 37˚C. The digestion was stopped by adding TFA to a concentration of 0.5%. Salt and buffer components were removed by in-house stage tips equipped with C18 resin[48]and the peptides dissolved in 0.1 % formic acid. The samples were analyzed on a Q-Exactive mass spectrometer as described earlier[49].

MS Data analysis

MS raw files were transformed into *.mgf files using the MS convert software. These files were analyzed using the MASCOT search engine (Matrix Science). Searches were performed against the UniProt database (version 06/2017 containing 554515 sequences) and an in-house database (http://www.medkem.gu.se/mucinbiology/databases/index.html) containing all human and mouse mucin sequences. Searches were performed with the following parameters: mass tolerance for the precursor ion of 5 ppm; tolerance for fragment ions 0.2 Da; full specificity for trypsin/AspN with a maximum of two missed cleavages; carbamidomethylation as static modification and oxidation of methionine as variable modification.

TGM-catalysed cross-linked peptides were searched using the StavroX software tool (version 3.6.6)[50] against theoretical intra- and intermolecular isopeptide cross-linked (di)peptides of the murine MUC2 using the following parameters: mass tolerance for the precursor ion of 2 ppm; tolerance for fragment ions 20 ppm; full specificity for trypsin/AspN with a maximum of three missed cleavages; Gln and Lys as cross-linking sites; composition of the cross-link $-NH_3$; carbamidomethylation as static modification and methionine oxidation as variable modification. Label-free mass spectrometric quantification of TGM isozymes was performed as recently described[20].

Data availability

The proteomics data set for label-free quantification used has been published[20] and deposited to the ProteomeXchange Consortium (http://proteomecentral.proteomexchange.org) with the dataset identifier PXD011527. The bulk RNA-seq data (GSE144363) are deposited in GEO and belong to the superserie GSE144436[20].

Statistical analysis

Statistical analyses were performed using the Prism software (version 9.0.1; GraphPad). Body weight and colon length were compared using the unpaired t-test with Welch`s correction. DAI scores were compared by multiple unpaired t-tests using the Holm-Sidák correction. Significance was accepted when p values were below 0.05. Data are expressed as mean ± standard deviation.

Acknowledgements

We acknowledge Ludvig Sollid, University of Oslo and Eleonara Candi, University of Rome for providing the *Tgm2*$^{-/-}$ and *Tgm3*$^{-/-}$ mice strains. This work was supported by the European Research Council ERC (694181), National Institute of Allergy and Infectious Diseases (U01AI095473, the content is solely the responsibility of the authors and does not necessarily represent the official views of the NIH), The Knut and Alice Wallenberg Foundation (2017.0028), Swedish Research Council (2017-00958), The Swedish Cancer Foundation (CAN 2017/360), IngaBritt and Arne Lundberg Foundation (2018-0117), Sahlgren's University Hospital (ALFGBG-440741, The ALF agreement 236501), Bill and Melinda Gates Foundation (OPP1202459), Wilhelm and Martina Lundgren's Foundation.

Author contributions

JDAS performed experiments and analyzed data; BD performed experiments and analyzed data; EELN performed experiments and analyzed data, LA performed experiments and analyzed data; GMHB performed experiments and analyzed data; BMA performed experiments and analyzed data; MEVJ data analysis; GCH conceptualized the study, analyzed data; CVR conceptualized the study, performed experiments and analyzed data. GCH and CVR wrote the paper. All authors reviewed the paper and accepted the final version.

Competing interests

The authors declare no competing interests.

References

1. Johansson, M.E. & Hansson, G.C. Immunological aspects of intestinal mucus and mucins. *Nat Rev Immunol* **16**, 639-649 (2016).
2. Rodriguez-Pineiro, A.M. *et al.* Studies of mucus in mouse stomach, small intestine, and colon. II. Gastrointestinal mucus proteome reveals Muc2 and Muc5ac accompanied by a set of core proteins. *Am J Physiol Gastrointest Liver Physiol* **305**, G348-356 (2013).
3. Atuma, C., Strugala, V., Allen, A. & Holm, L. The adherent gastrointestinal mucus gel layer: thickness and physical state in vivo. *Am J Physiol Gastrointest Liver Physiol* **280**, G922-929 (2001).
4. Johansson, M.E. *et al.* The inner of the two Muc2 mucin-dependent mucus layers in colon is devoid of bacteria. *Proc Natl Acad Sci U S A* **105**, 15064-15069 (2008).
5. Van der Sluis, M. *et al.* Muc2-deficient mice spontaneously develop colitis, indicating that MUC2 is critical for colonic protection. *Gastroenterology* **131**, 117-129 (2006).
6. Velcich, A. *et al.* Colorectal cancer in mice genetically deficient in the mucin Muc2. *Science* **295**, 1726-1729 (2002).
7. van der Post, S. *et al.* Structural weakening of the colonic mucus barrier is an early event in ulcerative colitis pathogenesis. *Gut* **68**, 2142-2151 (2019).
8. Svensson, F., Lang, T., Johansson, M.E.V. & Hansson, G.C. The central exons of the human MUC2 and MUC6 mucins are highly repetitive and variable in sequence between individuals. *Sci Rep* **8**, 17503 (2018).
9. Hansson, G.C. Mucins and the Microbiome. *Annu Rev Biochem* **89**, 769-793 (2020).
10. Godl, K. *et al.* The N terminus of the MUC2 mucin forms trimers that are held together within a trypsin-resistant core fragment. *The Journal of biological chemistry* **277**, 47248-47256 (2002).
11. Javitt, G. *et al.* Assembly Mechanism of Mucin and von Willebrand Factor Polymers. *Cell* **183**, 717-729 e716 (2020).

12. Recktenwald, C.V. & Hansson, G.C. The Reduction-insensitive Bonds of the MUC2 Mucin Are Isopeptide Bonds. *The Journal of biological chemistry* **291**, 13580-13590 (2016).
13. Lorand, L. & Graham, R.M. Transglutaminases: crosslinking enzymes with pleiotropic functions. *Nat Rev Mol Cell Biol* **4**, 140-156 (2003).
14. Folk, J.E. & Finlayson, J.S. The epsilon-(gamma-glutamyl)lysine crosslink and the catalytic role of transglutaminases. *Adv Protein Chem* **31**, 1-133 (1977).
15. Eckert, R.L. *et al.* Transglutaminase regulation of cell function. *Physiol Rev* **94**, 383-417 (2014).
16. Adamczyk, M., Griffiths, R., Dewitt, S., Knauper, V. & Aeschlimann, D. P2X7 receptor activation regulates rapid unconventional export of transglutaminase-2. *J Cell Sci* **128**, 4615-4628 (2015).
17. Siegel, M. *et al.* Extracellular transglutaminase 2 is catalytically inactive, but is transiently activated upon tissue injury. *PLoS One* **3**, e1861 (2008).
18. Telci, D. & Griffin, M. Tissue transglutaminase (TG2)--a wound response enzyme. *Front Biosci* **11**, 867-882 (2006).
19. Eckert, R.L., Sturniolo, M.T., Broome, A.M., Ruse, M. & Rorke, E.A. Transglutaminase function in epidermis. *J Invest Dermatol* **124**, 481-492 (2005).
20. Nystrom, E.E.L. *et al.* An intercrypt subpopulation of goblet cells is essential for colonic mucus barrier function. *Science* **372** (2021).
21. Sugimura, Y. *et al.* Screening for the preferred substrate sequence of transglutaminase using a phage-displayed peptide library: identification of peptide substrates for TGASE 2 and Factor XIIIA. *The Journal of biological chemistry* **281**, 17699-17706 (2006).
22. Yamane, A. *et al.* Identification of a preferred substrate peptide for transglutaminase 3 and detection of in situ activity in skin and hair follicles. *FEBS J* **277**, 3564-3574 (2010).
23. Axelsson, M.A., Asker, N. & Hansson, G.C. O-glycosylated MUC2 monomer and dimer from LS 174T cells are water-soluble, whereas larger MUC2 species formed early during biosynthesis are insoluble and contain nonreducible intermolecular bonds. *The Journal of biological chemistry* **273**, 18864-18870 (1998).
24. Kasdorf, B.T. *et al.* Mucin-Inspired Lubrication on Hydrophobic Surfaces. *Biomacromolecules* **18**, 2454-2462 (2017).
25. Johansson, M.E. *et al.* Bacteria penetrate the inner mucus layer before inflammation in the dextran sulfate colitis model. *PLoS One* **5**, e12238 (2010).
26. Jeong, E.M. *et al.* Transglutaminase 2 is dispensable but required for the survival of mice in dextran sulfate sodium-induced colitis. *Exp Mol Med* **48**, e267 (2016).
27. Stamnaes, J., Iversen, R., du Pre, M.F., Chen, X. & Sollid, L.M. Enhanced B-Cell Receptor Recognition of the Autoantigen Transglutaminase 2 by Efficient Catalytic Self-Multimerization. *PLoS One* **10**, e0134922 (2015).
28. Gross, S.R., Balklava, Z. & Griffin, M. Importance of tissue transglutaminase in repair of extracellular matrices and cell death of dermal fibroblasts after exposure to a solarium ultraviolet A source. *J Invest Dermatol* **121**, 412-423 (2003).
29. Yildiz, H.M., Speciner, L., Ozdemir, C., Cohen, D.E. & Carrier, R.L. Food-associated stimuli enhance barrier properties of gastrointestinal mucus. *Biomaterials* **54**, 1-8 (2015).
30. Di Maio, S. & Carrier, R.L. Gastrointestinal contents in fasted state and post-lipid ingestion: in vivo measurements and in vitro models for studying oral drug delivery. *J Control Release* **151**, 110-122 (2011).
31. Wongdee, K., Rodrat, M., Teerapornpuntakit, J., Krishnamra, N. & Charoenphandhu, N. Factors inhibiting intestinal calcium absorption: hormones and luminal factors that prevent excessive calcium uptake. *J Physiol Sci* **69**, 683-696 (2019).
32. Ahvazi, B., Kim, H.C., Kee, S.H., Nemes, Z. & Steinert, P.M. Three-dimensional structure of the human transglutaminase 3 enzyme: binding of calcium ions changes structure for activation. *EMBO J* **21**, 2055-2067 (2002).

33. Ahvazi, B., Boeshans, K.M., Idler, W., Baxa, U. & Steinert, P.M. Roles of calcium ions in the activation and activity of the transglutaminase 3 enzyme. *The Journal of biological chemistry* **278**, 23834-23841 (2003).
34. Yoo, S.H. Secretory granules in inositol 1,4,5-trisphosphate-dependent Ca2+ signaling in the cytoplasm of neuroendocrine cells. *FASEB J* **24**, 653-664 (2010).
35. Cheng, T. *et al.* Cystatin M/E is a high affinity inhibitor of cathepsin V and cathepsin L by a reactive site that is distinct from the legumain-binding site. A novel clue for the role of cystatin M/E in epidermal cornification. *The Journal of biological chemistry* **281**, 15893-15899 (2006).
36. Walden, M., Crow, A., Nelson, M.D. & Banfield, M.J. Intramolecular isopeptide but not internal thioester bonds confer proteolytic and significant thermal stability to the S. pyogenes pilus adhesin Spy0125. *Proteins* **82**, 517-527 (2014).
37. Hagan, R.M. *et al.* NMR spectroscopic and theoretical analysis of a spontaneously formed Lys-Asp isopeptide bond. *Angew Chem Int Ed Engl* **49**, 8421-8425 (2010).
38. Wu, F. & Chakravarti, S. Differential expression of inflammatory and fibrogenic genes and their regulation by NF-kappaB inhibition in a mouse model of chronic colitis. *J Immunol* **179**, 6988-7000 (2007).
39. Lyons, J. *et al.* Integrated in vivo multiomics analysis identifies p21-activated kinase signaling as a driver of colitis. *Sci Signal* **11** (2018).
40. Bognar, P. *et al.* Reduced inflammatory threshold indicates skin barrier defect in transglutaminase 3 knockout mice. *J Invest Dermatol* **134**, 105-111 (2014).
41. De Laurenzi, V. & Melino, G. Gene disruption of tissue transglutaminase. *Mol Cell Biol* **21**, 148-155 (2001).
42. Frezza, V. *et al.* Transglutaminase 3 Protects against Photodamage. *J Invest Dermatol* **137**, 1590-1594 (2017).
43. Trigwell, S.M., Lynch, P.T., Griffin, M., Hargreaves, A.J. & Bonner, P.L. An improved colorimetric assay for the measurement of transglutaminase (type II) -(gamma-glutamyl) lysine cross-linking activity. *Anal Biochem* **330**, 164-166 (2004).
44. Gustafsson, J.K. *et al.* An ex vivo method for studying mucus formation, properties, and thickness in human colonic biopsies and mouse small and large intestinal explants. *Am J Physiol Gastrointest Liver Physiol* **302**, G430-438 (2012).
45. Birchenough, G.M., Nystrom, E.E., Johansson, M.E. & Hansson, G.C. A sentinel goblet cell guards the colonic crypt by triggering Nlrp6-dependent Muc2 secretion. *Science* **352**, 1535-1542 (2016).
46. Friedman, D.J. *et al.* From the Cover: CD39 deletion exacerbates experimental murine colitis and human polymorphisms increase susceptibility to inflammatory bowel disease. *Proc Natl Acad Sci U S A* **106**, 16788-16793 (2009).
47. Schulz, B.L., Packer, N.H. & Karlsson, N.G. Small-scale analysis of O-linked oligosaccharides from glycoproteins and mucins separated by gel electrophoresis. *Anal Chem* **74**, 6088-6097 (2002).
48. Rappsilber, J., Ishihama, Y. & Mann, M. Stop and go extraction tips for matrix-assisted laser desorption/ionization, nanoelectrospray, and LC/MS sample pretreatment in proteomics. *Anal Chem* **75**, 663-670 (2003).
49. Fernandez-Blanco, J.A. *et al.* Attached stratified mucus separates bacteria from the epithelial cells in COPD lungs. *JCI Insight* **3** (2018).
50. Gotze, M. *et al.* StavroX--a software for analyzing crosslinked products in protein interaction studies. *J Am Soc Mass Spectrom* **23**, 76-87 (2012).

762 **Figure Legends**

763

764 **Figure 1: mRNA expression, protein abundance, and spatial localization of TGM**
765 **isozymes in the large intestine.**

766 (**a**) mRNA-seq expression data of the goblet cell and non-goblet cell fraction from a reporter
767 mouse strain expressing fluorescently-labelled MUC2. Goblet cells were separated from
768 other epithelial cell types using FACS-mediated cell sorting[20]. The graph shows the
769 normalized expression levels of the transglutaminase family members *Tgm*1-7 and *F13a1* in
770 the goblet cell and non-goblet cell fraction. Four biological replicates were analyzed.
771 (**b**) Label-free relative quantification of TGM isozymes 2 and 3 in goblet cell and remaining
772 epithelial cells after FACS-mediated cell sorting from RedMUC2^{98trTg} mice[20]. After protein
773 extraction, the abundance of TGM2 and 3 in the two fractions was measured by mass
774 spectrometry and the data analyzed using the MaxQuant software. Four biological replicates
775 were analyzed.
776 (**c**) Confocal microscopy of large intestinal tissue specimens from C57/BL6, *Tgm3*$^{-/-}$ and
777 *Tgm2*$^{-/-}$ mice suggests no TGM2 biosynthesis in the colon. The sections were probed with a
778 monoclonal antibody against TGM2 followed by detection with a secondary antibody
779 coupled to Alexa Fluor 647 (red) and sections counterstaining with the UEA1 lectin coupled
780 to rhodamine (green) for goblet cell and mucus visualization. Nuclei are shown in grey and
781 were visualized using the Sytox green stain. The scale bar corresponds to 20 μm. Images are
782 representative of three biological replicates.
783 (**d**) Analogously, confocal microscopy of colon specimen from C57/BL6, *Tgm3*$^{-/-}$ and *Tgm2*$^{-/-}$
784 mice analyzed for TGM3 (red) using a polyclonal anti-TGM3 antibody that was detected by a
785 secondary antibody coupled to Alexa 647 indicating TGM3 biosynthesis in WT and *Tgm2*$^{-/-}$

mice. UEA1 (green) and Hoechst (grey) were used for counterstaining. Images are representative of three biological replicates. The scale bar corresponds to 20 μm.

(**e**) Protein abundance analysis of TGM isoforms by Western blot in colonic mucus. The supernatant of precipitated mucus was analyzed for the presence of TGM2 and 3 using a monoclonal anti-TGM2 antibody and a polyclonal anti-TGM3 antibody. Goat anti-mouse IgG1-isoform antibody coupled to an IR680 dye and anti-rabbit IgGs coupled to an IR790 dye were used for visualization on a LI-COR Odyssey Clx workstation. Recombinant non-activated or calcium-activated TGM2 and 3 were loaded as positive controls. The red dashed line marks the IgG1 heavy chain (IgG1-HC) recognized by the secondary antibody against the TGM2 antibody and served as loading control. A representative analysis with three biological replicates per mouse strain is shown.

Figure 2: Qualitative, quantitative and *ex vivo* analysis of extracellular transglutaminase activity.

(**a**) Qualitative determination of calcium-induced transglutaminase activity in colonic mucus samples. Samples from the indicated strains were spiked with biotinylated TGM2 (T26) and TGM3 (E51) selective acyl-acceptor peptide substrates and with calcium addition in the absence or presence of IAA followed by incubation for one hour at 37˚C. The reaction products were separated by SDS-PAGE and subsequently visualized by Western blot using streptavidin labelled with an IR680LT-dye on a LiCOR Odyssee Clx imager. Non-specific signals from endogeneously biotinylated proteins were marked with a triangle. A representative example of three biological replicates per mouse strain is shown.

(**b**) Qualitative determination of intrinsic transglutaminase activity in colonic mucus samples. Samples from the indicated strains were supplied with biotinylated TGM2 (T26) and TGM3-(E51) specific acyl-acceptor peptide substrates without calcium addition in the absence or

presence of IAA and incubated for one hour at 37˚C. The reaction products were separated by SDS-PAGE followed by Western blot detection using streptavidin labelled with an IR680LT-dye. Non-specific signals from endogeneously biotinylated proteins were marked with a triangle.A representative example of three biological replicates per mouse strain is shown.

(**c**) Detection of putative acyl-acceptor proteins in mucus. Mucus samples from the different mouse strains were incubated in the presence of 5-Bioinyl-pentylamine (5-BP) for one hour at 37˚C. Control reactions were performed in the presence of IAA for the visualization of false-positive signals. The incorporation of 5-BP was detected by Western Blot using streptavidin labelled with an IR680LT-dye. Non-specific signals from endogeneously biotinylated proteins were marked with a triangle. A representative example of three biological replicates per mouse strain is shown.

(**d**) Quantitative determination of transglutaminase activity in colonic mucus samples. TGM activity in mucus from the different mouse strains was determined by the incorporation of TGM2 (T26) and TGM3 (E51) specific peptide substrates or a promiscuous TGM acyl-acceptor peptide (A25) into casein as described under materials and methods. The respective cross-linking activity in the samples was calculated from the calibration curve of the recombinant activated TGM standards and subsequently normalized against the protein concentration of the samples. At least four biological replicates per substrate and mouse strain were analyzed.

(**e**-**h**) *Ex vivo* analysis of transglutaminase activity. Tissues were mounted in a perfusion chamber as illustrated (**e**) and transglutaminase activity probed with the glutamine-donor peptide E51 coupled to FITC (magenta) for 30 minutes at 37˚C. After washing away non-incorporated peptide the tissue specimen were analyzed by confocal microscopy. Mucus and nuclei were counterstained with the UEA1 lectin coupled to rhodamine (green) and the Hoechst stain (blue) respectively. The top panels show Z-stacks of the explant with (left) or

without (right) the UEA1 counterstain. The bottom panels show x/y projections of the indicated area from the respective Z-stack on top. Colonic specimen from WT mice (**f**), *Tgm3*$^{-/-}$ mice (**g**) or WT mice in the presence of the pan-TGM inhibitor Z-DON (**h**) were probed for E51 incorporation. The scale bar corresponds to 50 µm. Three animals per mouse strain were analyzed.

Figure 3: Loss of TGM3 causes biochemical alterations of mucus and MUC2.

(**a**) Schematic figure of the human and mouse MUC2 domain structure. The domains of the complete sequence excluding the signal sequence are shown. The abbreviations correspond to vWD, von-Willebrand D domain; CysD, Cystein-rich domain; PTS, Proline, Serine, Threonine-rich domain that after *O*-glycosylation becomes a mucin domain; vWC, von-Willebrand C domain; CK, Cysteine-knot domain.

(**b**) MUC2 mono- and oligomers from WT, *Tgm2*$^{-/-}$, and *Tgm3*$^{-/-}$ colonic mucus were separated by composite AgPAGE and stained by in-gel immunodetection using a polyclonal anti-MUC2-C3 (Genentech) and secondary antibody coupled to the AlexaFlour790-dye on an Odyssey Clx workstation.

(**c**) Limited Proteolysis of MUC2 by the serine protease Lys-C. Mucus samples from the indicated mouse strains were incubated in the absence or presence of Lys-C for 90 minutes at 25˚C and the reaction products separated via composite AgPAGE followed by visualization of MUC2 with Alcian Blue.

(**d**) Heat map of the sequence coverage of MUC2 domains. The color coded sequence coverage of the different MUC2 domains from three biological replicates of non-treated MUC2 monomers from mucus samples of WT (WT-M) and *Tgm3*$^{-/-}$ (*Tgm3*$^{-/-}$-M) animals as indicated in Fig. 3c are shown. The various MUC2 domains are placed from the N-terminus (top) to the C-terminus (bottom) on the ordinate. Only peptides with an ion score >25 were

taken into consideration. The two PTS domains were excluded as they are due to their high glycosylation heterogeneity not analyzable.

(**e**) Detection of transglutaminase reaction products. Example of an isopeptide dipeptide cross-link that was solely detected in MUC2 from WT animals. MS2 fragment spectrum of the parent ion $[M+2H]^{2+}$ 775.44 is shown. B ions are labelled in red and y ions in blue. The prarent ion is labelled in green.

(**f**) Analysis of MUC2 polymerisation. Mucus samples from WT and the TGM knock-out strains and their protein concentrations adjusted to 1 mg/ml. After centrifugation (1,000 x g, 30 minutes, 4˚C), precipitating the insoluble MUC2, the absorbance for soluble material was recorded at 600 nm. Three biological replicates per strain were analyzed.

(**g**) Hydrophobicity analysis of mucus from WT and *Tgm3*$^{-/-}$ mice. Mucus samples were adjusted to a protein concentration 1 mg/ml in TBS. SyproOrange was added and the melting curve of the samples analyzed by increasing the temperature by 0.5˚C every 30 seconds from 25˚C to 99˚C in a thermocycler. The fluorescence change was recorded every 30 seconds and subsequently normalized by subtraction of the buffer control fluorescence for each data point. For rescuing the WT behavior, 1 U of activated recombinant TGM3 was added to mucus from *Tgm3*$^{-/-}$ animals and the samples incubated for 60 minutes at 37˚C. Afterwards the cross-linking activity was inhibited with IAA before adding SyproOrange. The graph shows the arithmetic average of three biological replicates.

(**h-i**) Pronase-treatment of distal colon specimen from WT (**h**) and *Tgm3*$^{-/-}$ (**i**) mice. Colonic explants from WT and *Tgm3*$^{-/-}$ mice were mounted in a chamber and pronase in Krebs-buffer was added before examination under a confocal microscope as sketched in Fig. 2e. The mucus surface was visualized by placing fluorescently labelled beads with a diameter of one µm on top of the mucus layer and the epithelium counterstained using the Syto 9 stain. The top panel shows the isosurfaces of the tissue and of the individual beads over time. The white

scale bar corresponds to 50 µm. The lower panel shows the distribution of the fluorescently-labelled beads in relation to the tissue surface as violin plot where the black bar marks the median of bead distance from the epithelium. Three animals per mouse strain were analysed. OM=outer (loose) mucus layer, IM=inner mucus layer.

Figure 4: Dextran sodium sulfate treatment shows decreased mucus protection.

WT and Tgm3-/- mice were cohoused and supplied via drinking water with 3% (w/v) dextran sodium sulfate.

(**a**) Body weight change of DSS-treated mice over time. The body weight of the mice was recorded once per day throughout the whole experiment and the change in body weight respective to the starting body weight of both groups plotted against the time. The graph shows the comparison of one litter per strain consisting of five animals in each group.

(**b**) Detection of occult blood in feces. Fecal samples were collected from the DSS-treated animals and analyzed for hidden blood using a hemoccult kit as described in materials and methods. The mean ratio of hemoccult-positive samples from each group was plotted against time. The graph shows the comparison of one litter per strain consisting of five animals in each group.

(**c**) The disease activity index (DAI) was determined as sum of the changes in body weight, stool consistency, rectal bleeding for every animal for the indicated time points and the mean with standard deviation for the both groups plotted against the time. *$p<0.05$. The graph shows the comparison of one litter per strain consisting of five animals in each group.

(**d**) Survival analysis of DSS-treated mice. The probability of survival was calculated using the GraphPad prism software. Mice were sacrificed when the initial body weight loss exceeded 10%. The graph shows the summary of the two litters per strain that were analysed independently and represents ten animals in each group.

(**e-f**) Colon length changes of DSS-treated WT and *Tgm3*$^{-/-}$ mice. At day 8 or at the ethical endpoint, animals were sacrificed and the colon length of each animal measured. A representative colon of WT and *Tgm3*$^{-/-}$ animals is shown in (**e**). (**f**) Normalized colon length of DSS-treated WT and *Tgm3*$^{-/-}$ mice. The graph shows the summary of the two litters per strain that were analysed independently and represents ten animals in the WT and nine animals in the *Tgm3*$^{-/-}$ group. $p<0.001$.

(**g**) Histological analysis of DSS-treated WT and *Tgm3*$^{-/-}$ mice. Representative Alcian Blue-Periodic Acid Schiff-stained sections from proximal (PC) and distal colon (DC) of WT and TGM3-deficient animals are shown. The black scale bar on the left corresponds to 100 μm.

(**h**) Immunohistochemical analysis of WT and *Tgm3*$^{-/-}$ mice for the presence of TGM2 after DSS treatment. Tissue specimen from WT and *Tgm3*$^{-/-}$ animals were probed with a monoclonal anti-TGM2 antibody (red) and the UEA1 lectin (green). Nuclei were stained using the Hoechst stain (grey). The white scale bar on the right corresponds to 30 μm.

Figure 1

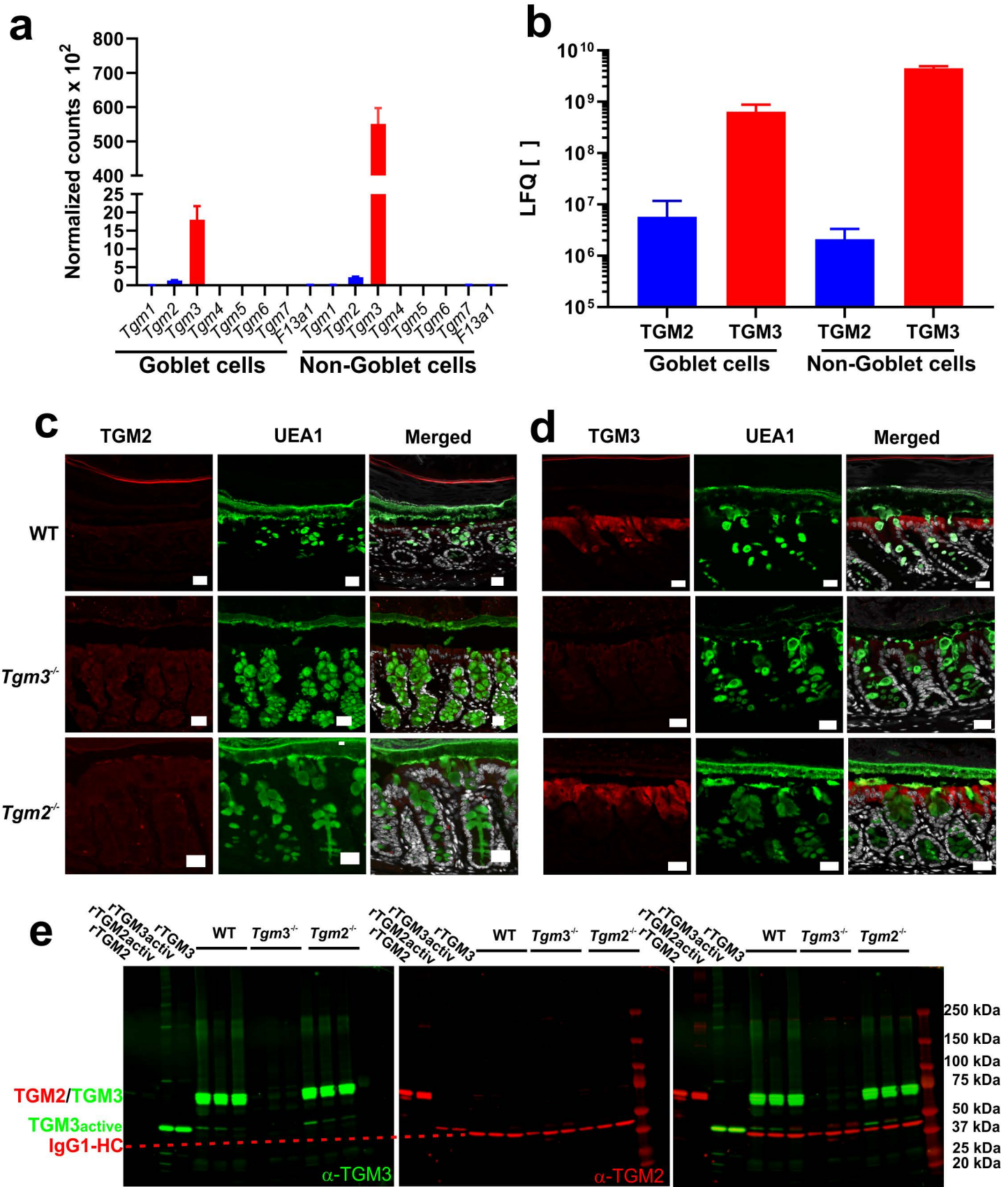
a
Normalized counts x 10²
800
700
600
500
400
25
20
15
10
5
0
Tgm1
Tgm2
Tgm3
Tgm4
Tgm5
Tgm6
Tgm7
F13a1
Tgm1
Tgm2
Tgm3
Tgm4
Tgm5
Tgm6
Tgm7
F13a1
Goblet cells
Non-Goblet cells
b
LFQ [ ]
10¹⁰
10⁹
10⁸
10⁷
10⁶
10⁵
TGM2
TGM3
TGM2
TGM3
Goblet cells
Non-Goblet cells
c
TGM2
UEA1
Merged
WT
Tgm3-/-
Tgm2-/-
d
TGM3
UEA1
Merged
e
rTGM2
rTGM2activ
rTGM3
rTGM3activ
WT
Tgm3-/-
Tgm2-/-
TGM2/TGM3
TGM3active
IgG1-HC
α-TGM3
α-TGM2
250 kDa
150 kDa
100 kDa
75 kDa
50 kDa
37 kDa
25 kDa
20 kDa

Figure 2

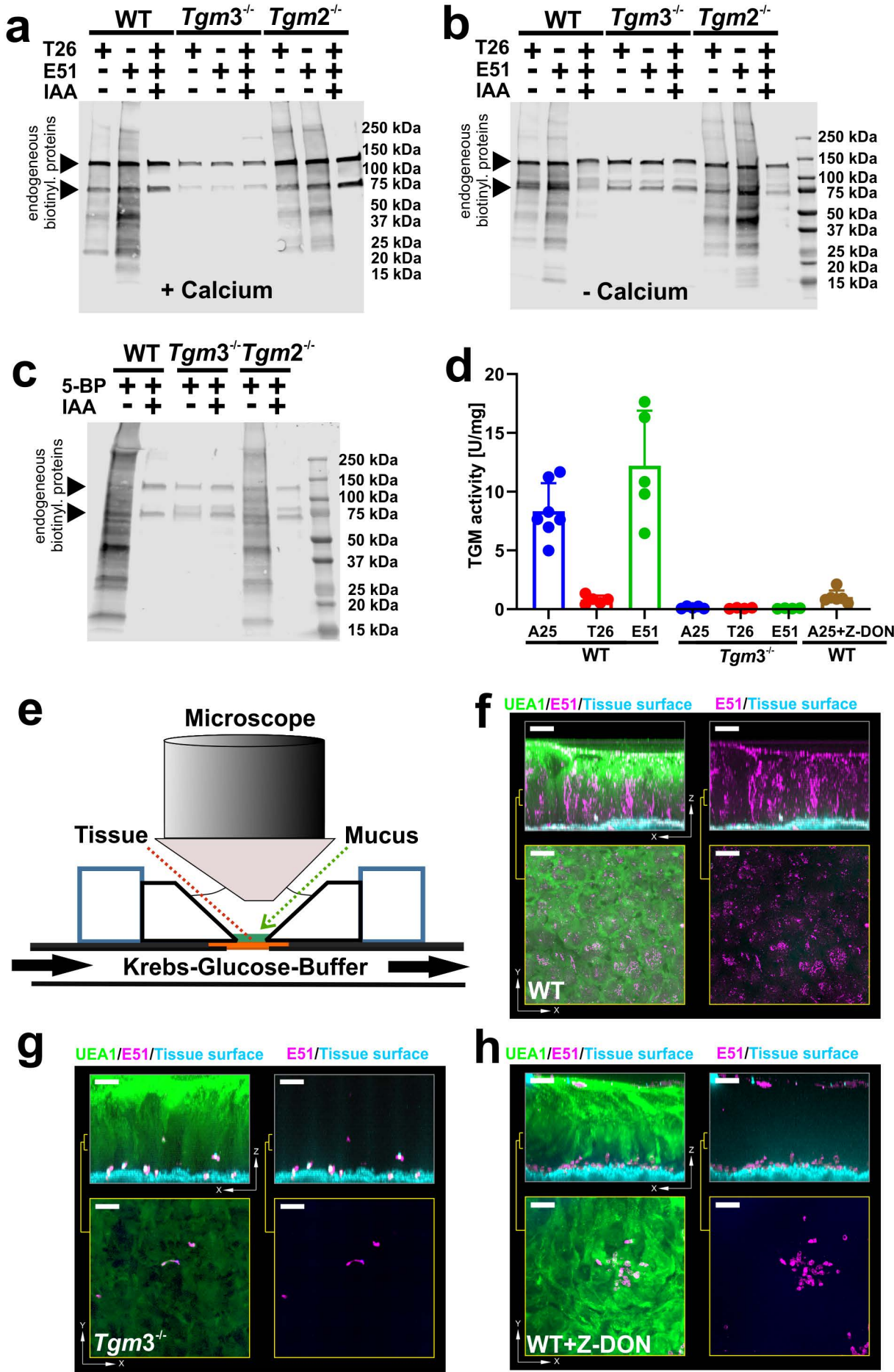
a
WT
Tgm3-/-
Tgm2-/-
T26
E51
IAA
endogeneous biotinyl. proteins
250 kDa
150 kDa
100 kDa
75 kDa
50 kDa
37 kDa
25 kDa
20 kDa
15 kDa
+ Calcium
b
- Calcium
c
5-BP
d
TGM activity [U/mg]
A25
T26
E51
A25+Z-DON
e
Microscope
Tissue
Mucus
Krebs-Glucose-Buffer
f
UEA1/E51/Tissue surface
E51/Tissue surface
WT
g
Tgm3-/-
h
WT+Z-DON

Figure 3

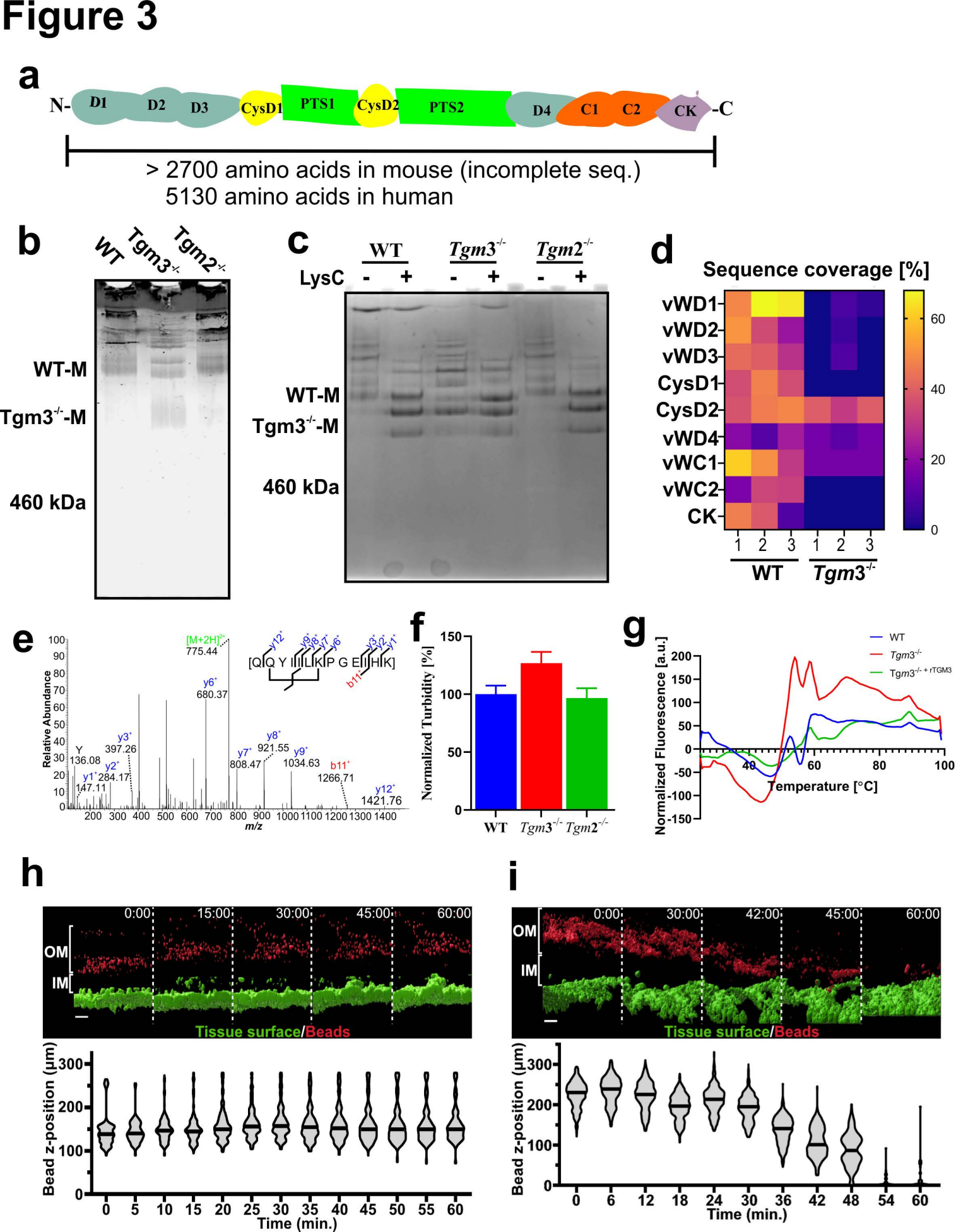
a
N-
D1
D2
D3
CysD1
PTS1
CysD2
PTS2
D4
C1
C2
CK
-C
> 2700 amino acids in mouse (incomplete seq.)
5130 amino acids in human
b
WT
Tgm3-/-
Tgm2-/-
WT-M
Tgm3-/--M
460 kDa
c
WT
Tgm3-/-
Tgm2-/-
LysC - + - + - +
WT-M
Tgm3-/--M
460 kDa
d
Sequence coverage [%]
vWD1
vWD2
vWD3
CysD1
CysD2
vWD4
vWC1
vWC2
CK
1 2 3 1 2 3
WT
Tgm3-/-
60
40
20
0
e
Relative Abundance
m/z
[M+2H]2+
775.44
[Q Q Y I I L K P G E I H K]
y12+
y9+
y8+
y7+
y6+
y3+
y2+
y1+
b11+
Y
136.08
y3+
397.26
y2+
284.17
y1+
147.11
y6+
680.37
y8+
921.55
y7+
808.47
y9+
1034.63
b11+
1266.71
y12+
1421.76
f
Normalized Turbidity [%]
WT
Tgm3-/-
Tgm2-/-
g
Normalized Fluorescence [a.u.]
Temperature [°C]
WT
Tgm3-/-
Tgm3-/- + rTGM3
h
0:00
15:00
30:00
45:00
60:00
OM
IM
Tissue surface/Beads
Bead z-position (µm)
Time (min.)
i
0:00
30:00
42:00
45:00
60:00
OM
IM
Tissue surface/Beads
Bead z-position (µm)
Time (min.)

Figure 4

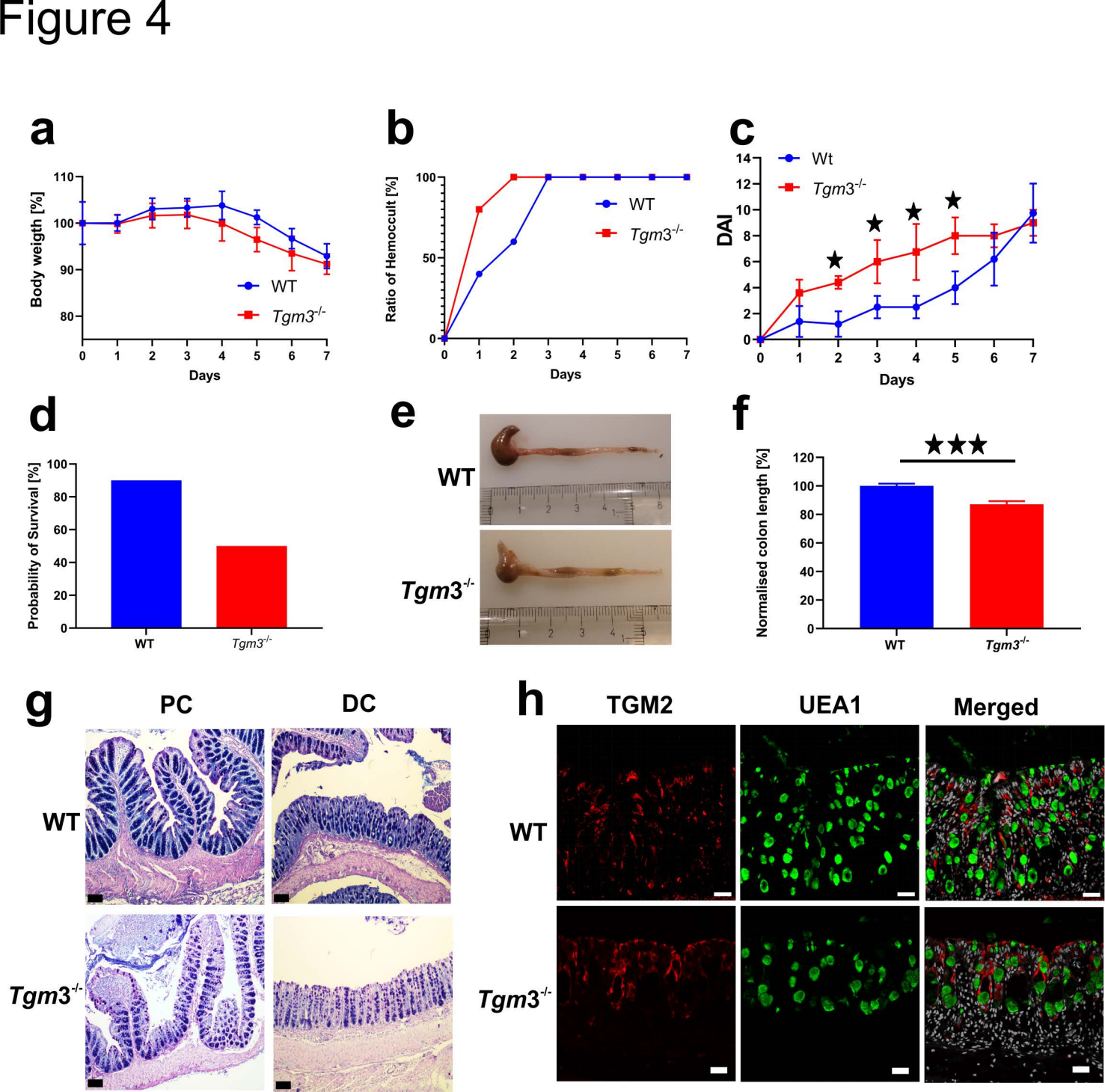
a
Body weigth [%]
110
100
90
80
0 1 2 3 4 5 6 7
Days
WT
Tgm3-/-
b
Ratio of Hemoccult [%]
100
50
0
0 1 2 3 4 5 6 7
Days
WT
Tgm3-/-
c
DAI
14
12
10
8
6
4
2
0
0 1 2 3 4 5 6 7
Days
Wt
Tgm3-/-
d
Probability of Survival [%]
100
80
60
40
20
0
WT
Tgm3-/-
e
WT
Tgm3-/-
f
Normalised colon length [%]
120
100
80
60
40
20
0
WT
Tgm3-/-
g
PC
DC
WT
Tgm3-/-
h
TGM2
UEA1
Merged
WT
Tgm3-/-

Supplementary Files

This is a list of supplementary files associated with this preprint. Click to download.

- SupplementaryFiguresS14.pdf
- SupplementaryMovieM1.mp4
- SupplementaryMovieM2.mp4
- SupplementaryMovieM3.mp4